

Closing the gap between functional QCD method and experimental observables

Fei Gao

Beijing Institute of Technology, BIT, in fQCD collaboration

ECT*, Trento, May 24th, 2023



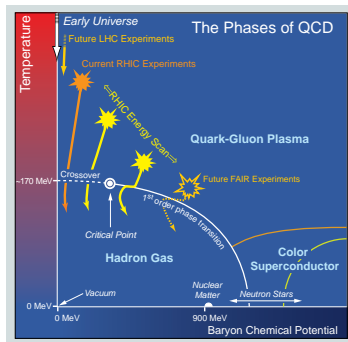
Outline

- 1 **Backgrounds**
- 2 **The truncation of functional QCD method and the up-to-date chiral phase diagram**
 - Framework of functional QCD method
 - Chiral phase diagram of QCD
- 3 **QCD Thermodynamic properties and its possible application**
 - QCD Thermodynamic properties
 - Determining the evolution of universe
- 4 **Summary**

Quantum ChromoDynamics

The phenomena of QCD can be mapped into one phase diagram:

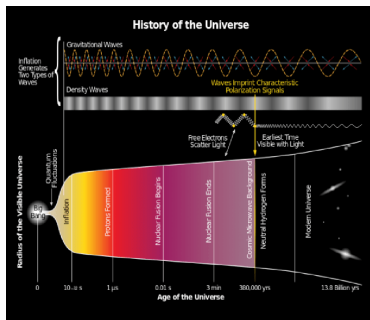
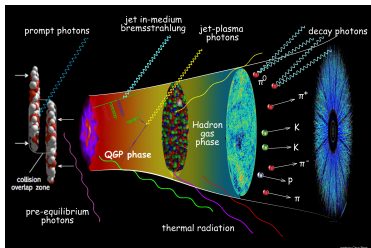
- quark-gluon plasma at high temperature and chemical potential
- Color-superconducting phase at low temperature and high baryon density
- The phase transition between the normal hadron phase and the quark-gluon plasma phase driven by different combination of temperature and chemical potential, and connected with crossover at low density by critical end point (CEP)



¹The frontiers of nuclear science, A long range plan[J]. 2008.

phenomena

QCD in heavy ion collision and Universe evolution:



Framework of functional QCD method

Dyson-Schwinger equations (DSEs) and functional renormalization group (fRG) approach are the nonperturbative approach in continuum QCD which contain the features of both confinement and chiral symmetry breaking.

DSEs are the equations of motions in quantum field theory:

$$\frac{\partial \mathcal{S}}{\partial \phi} = J$$

fRG is based on the idea of homotopy:

$$f(\lambda) = \int_0^\infty dx e^{-\lambda x^2} \rightarrow \frac{\partial f(\lambda)}{\partial \lambda} = - \int_0^\infty dx x^2 e^{-\lambda x^2} = - \frac{f(\lambda)}{2\lambda}$$

The truncation of the functional QCD methods

The truncation is required in functional QCD methods as the equations are not closed.

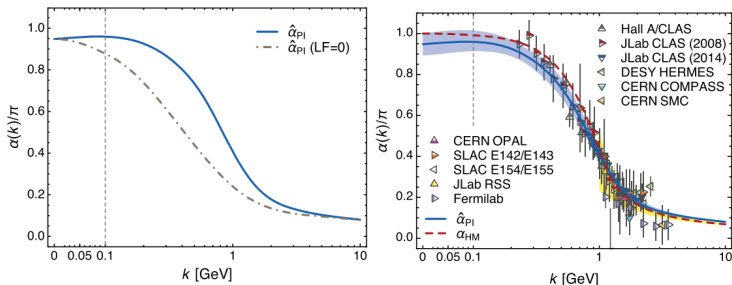
- How to generally evaluate the truncation?
- How to reduce the higher order correction and make the truncation controllable?

$$\left(\text{---} \circ \text{---} \right)^{-1} = \left(\text{---} \right)^{-1} + \underbrace{\text{---} \circ \text{---} \circ \text{---}}_{\Sigma(p)}$$

$$\text{---} \circ \text{---} = \text{---} \circ \text{---} + \text{---} \circ \text{---} \circ \text{---} + \text{---} \circ \text{---} \circ \text{---} \circ \text{---} + \dots$$

Effective Charge

The hints from effective charge:



- The running of the coupling can be partly captured by the running of two point functions (STIs)
- The efforts beyond props are "perturbative", and can be captured by the correction of vertex.

D. Binosi et al, PRD96, 054026 (2017); A. Aguilar et al, PRD80, 085018 (2009).

A. Deur et al, Prog. Part.Nucl. Phys. 90, 1 (2016);

AdS/CFT correspondence from fRG

fRG equation:

$$k\partial_k\Gamma_k = \frac{1}{2}\text{Tr}[k\partial_k R_k(p) \cdot G_k(p)] \equiv \beta_\Gamma$$

Identifying $k = 1/z$, the equation becomes Holographic equation:

$$\left(-\frac{d^2}{dz^2} - \frac{1-4L^2}{4z^2} + U_J(z)\right)\psi(z) = \mathcal{M}^2\psi(z)$$

$$U_J(z) = -\frac{z^{-1-\delta}}{\Gamma_z^{(n)}}\partial_z\left(z^\delta\beta_\Gamma^{(n)}\right)$$

¹FG, Masatoshi Yamada, PRD 106, 126003(2022).

The hints from the relation between fRG and holographic equation:

- AdS/CFT correspondence is hold through the fixed point since only there the potential can be uniquely determined.
- The bound states spectrum (Regge trajectory, etc) can be studied through AdS/CFT correspondence, and it is also a useful tool for studying phase transition(universality class).

The fixed point simplifies the truncation:

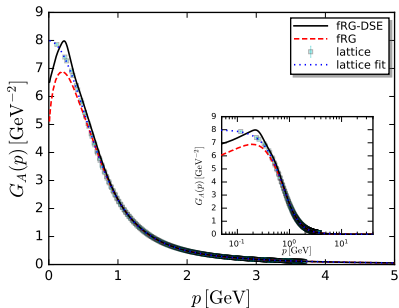
- The fixed point defines an "perturbative" expansion in infrared.
- Only the running of propagator and vertex is relevant.
- It is possible to construct a minimal truncation in quark gap equation which can describe both the vacuum and the finite T and μ physics (see Yi Lu's talk)

The baseline of the truncation:

The truncation that describes both the vacuum and the phase transition region requires:

- Describe the running mass of quark and gluon
- Describe the running of the coupling

The Yang-Mills sector is relatively separable:



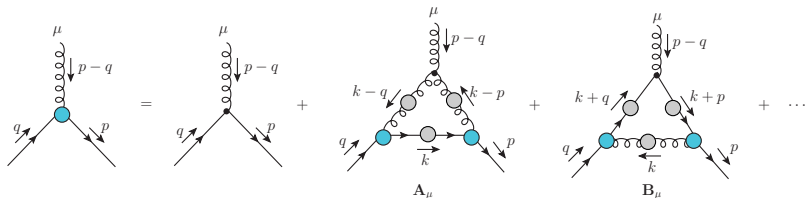
Lattice:

A. G. Duarte et al, PRD 94, 074502 (2016),
 P. Boucaud et al, PRD 98, 114515 (2018),
 S. Zafeiropoulos et al, PRL 122, 162002 (2019)

fRG:

W.-j. Fu et al, PRD 101, 054032 (2020)
 Cyrol, Fister, Mitter, Pawłowski, Strodthoff, PRD 94 (2016) 5,
 054005

Quark gluon vertex



With Landau gauge, only the transversally projection:

$$\Gamma^\mu(q, -p) = \sum_{i=1}^8 \lambda_i(q, -p) P^{\mu\nu}(q-p) \mathcal{T}_i^\nu(q, -p),$$

The three dominant components associated with

$$\mathcal{T}_1^\mu(p, q) = -i\gamma^\mu,$$

$$\mathcal{T}_4^\mu(p, q) = (\not{p} + \not{q})\gamma^\mu, \quad \mathcal{T}_7^\mu(p, q) = \frac{i}{2}[\not{p}, \not{q}]\gamma^\mu.$$

$O(4)$ symmetry approx. at finite T/μ is sometimes applied.

Quark gluon vertex

1. fRG assisted gap equation:

- **Input:** $N_f = 2$ gluon propagator and quark gluon vertex in vacuum from FRG (A. K. Cyrol, et al, Phys. Rev. D97, 054006 (2018)).

Difference-DSE: The gluon propagator and quark gluon vertex in finite temperature and chemical potential by computing the difference:

$$\Gamma^{(n)}(p) \Big|_{T, \mu_B, N_f} = \Gamma^{(n)}(p) \Big|_{0,0,2} + \Delta\Gamma^{(n)}(p).$$

Quark gluon vertex

Note that the couplings rely on the schemes and the approx. involved, and therefore,

2. Self-consistency condition:

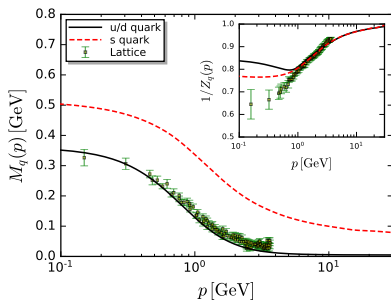
- Compute the running couplings in the present SDE setup with the input of gluon propagator, and adjust $\alpha_s(\mu)$ to match with the data of couplings
- Or simply employ the STI of the quark-gluon vertex:

$$\lambda_1(\bar{p}) = g_s(\mu)L_1(\bar{p}),$$

where L_1 is the solution of the STI for the classical tensor structure, and minimising the difference between the two sides singles out a unique $\alpha_s(\mu)$.

¹FG, J. Papavassiliou and J. M. Pawłowski, PRD103, 094013(2021).

Running mass of quark:

**lattice:**

P. O. Bowman et al, PRD71, 054507 (2005)

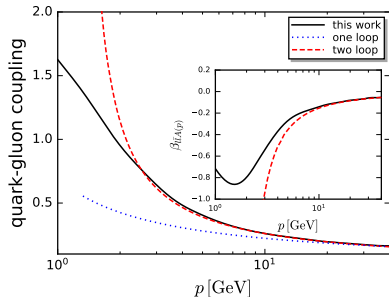
fRG:

W.-j. Fu et al, PRD 101, 054032 (2020)

fRG-DSE:

FG et al, PRD 102, 034027 (2020)

The running coupling coincides with 2 loop running till 3 GeV.

**DSE:**

FG, J. Papavassiliou, J. Pawłowski, PRD103, 094013(2021).

Towards the realistic phase structure of QCD

lattice QCD simulation:

- solid computations at vanishing chemical potential,
- due to the sign problem, it is difficult for lattice QCD to reach large chemical potential region.

Large chemical potential is accessible by functional QCD approaches.

For functional QCD method, the phase diagram of DCSB since the chiral phases is identified by quark propagator.

- chiral symmetry breaking phase: Nambu phase
- chiral symmetry preserved phase: Wigner phase

¹**FG** and Jan M. Pawłowski, PLB 820 (2021) 136584 .

²**FG** and Jan M. Pawłowski, PRD (2020) 102, 034027 .

QCD phase diagram

The Cornwall–Jackiw–Tomboulis (CJT) effective potential:

$$\Gamma(S) = -\text{Tr}[\ln(S_0^{-1}S) - S_0^{-1}S + 1] + \Gamma_2(S)$$

where S_0 and S stands for the bare and full quark propagator, Γ_2 is the 2PI contribution. Calculating the variation respective to quark propagator, we have:

$$\frac{\partial^2 \Gamma}{\partial S^2} = S^{-2} + \frac{\partial \Gamma_2(S)}{\partial S}$$

combing with the derivative on the quark propagator DSE as:

$$-S^{-2} \frac{\partial S}{\partial T} = 1 + \frac{\partial \Gamma_2(S)}{\partial S} \frac{\partial S}{\partial T}$$

The criterion is then given by¹:

$$\frac{\partial S}{\partial T} = -\frac{1}{\partial^2 \Gamma / \partial S^2}$$

¹FG, Yu-xin Liu. Phys. Rev. D 94 (2016) 7, 076009.

phase diagram

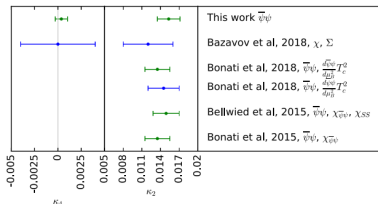
$$\frac{d(P_N - P_W)}{dT} = \left(\frac{\partial P_N}{\partial \mu} - \frac{\partial P_W}{\partial \mu} \right) \frac{\partial \mu}{\partial T} + \left(\frac{\partial P_N}{\partial T} - \frac{\partial P_W}{\partial T} \right) = 0.$$

Therefore, the phase transition line should bend down typically:

$$\frac{\partial \mu}{\partial T} = - \frac{s_N - s_W}{n_N - n_W} < 0.$$

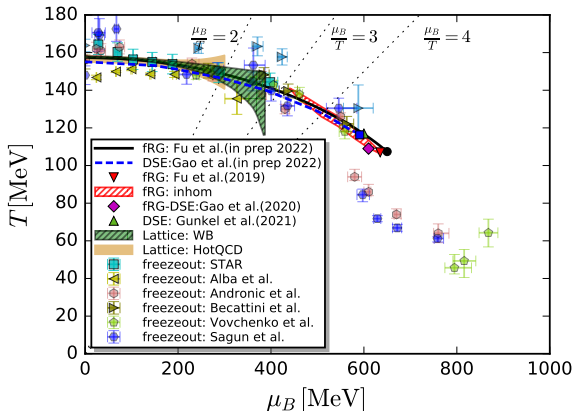
The line can be parametrized as:

$$\frac{T_c(\mu_B)}{T_c} = 1 - \kappa \left(\frac{\mu_B}{T_c} \right)^2 + \lambda \left(\frac{\mu_B}{T_c} \right)^4 + \dots,$$



QCD phase diagram

Phase diagram in temperature-chemical potential region for 2+1 flavour QCD



The fQCD computations of chiral phase transition are converging:

- $T_C = 155$ MeV and $\kappa \sim 0.16$
- Estimated range of CEP:
 $T \in (100, 110)$ MeV
 $\mu_B \in (600, 700)$ MeV
- $\sqrt{s_{NN}} \in 2 \sim 4$ GeV.

W.-j. Fu et al, PRD 101, 054032 (2020)
FG and Jan M. Pawłowski, PLB 820, 136584(2021)
P.J. Gunkel, C. S. Fischer, PRD 104, 054022 (2021).

- with no model parameters included
- subleading term: the hadron resonance channel

QCD thermodynamic properties

QCD thermodynamic properties

QCD EoS and related thermodynamic properties are important for numerous reasons:

- essential for our understanding of QCD matter.
- necessary for interpreting data collected at running and planned heavy-ion experiments as well as further predictions
- **explaining the evolution of the Universe.**

QCD thermodynamic properties

The obstacle for DSEs is that the effective potential is divergent and need to be subtracted of the vacuum energy to get the physical pressure.

Recalling the quark effective potential of QCD in the mean field approximation (with bare vertex and modelling interaction kernel), which is

$$P[S] = \frac{T}{V} \ln Z = \frac{T}{V} (\text{Tr} \text{Ln}[\beta S^{-1}] - \frac{1}{2} \text{Tr}[\Sigma S]), \quad (1)$$

If we put a free propagator in, we could get its analytic form

$$P(T) = 2 \int \frac{d^3 \vec{p}}{(2\pi)^3} [A + \omega + 2 \ln(1 + e^{-\beta \omega})], \quad (2)$$

where $\omega = \sqrt{\vec{p}^2 + m^2}$, A is a constant.

The first two terms bring in the divergence.

QCD thermodynamic properties

Considering such a relation of analytic continuation

(FG et al, PRD 93, 094019 (2016))

$$\begin{aligned}
 T \sum_{n=-\infty}^{\infty} f(p_0 = i\omega_n + \mu) &= \frac{1}{2\pi i} \int_{-i\infty}^{i\infty} dp_0 f(p_0) \\
 &+ \oint dp_0 f(p_0) - \frac{1}{2\pi i} \int_{-i\infty+\mu+\epsilon}^{i\infty+\mu+\epsilon} dp_0 f(p_0) \frac{1}{e^{(p_0-\mu)/T} + 1} \\
 &- \frac{1}{2\pi i} \int_{-i\infty+\mu-\epsilon}^{i\infty+\mu-\epsilon} dp_0 f(p_0) \frac{1}{e^{-(p_0-\mu)/T} + 1}. \quad (3)
 \end{aligned}$$

The subtraction scheme leads to a cutoff-independent result

(C. S. Fischer, Prog.Part.Nucl.Phys. 105 (2019) 1-60).

QCD thermodynamic properties

Currently, the functional QCD approaches can only calculate the quark potential directly, while the gluon sector still awaits further investigations.

One may incorporate the lattice QCD simulation at $\mu = 0$ here to combine the advantages of the two methods. One can calculate the quark number densities $\{n_q\}$ at finite chemical potential and obtain the pressure by:

$$P(T, \mu) = P_{Latt.}(T, \mathbf{0}) + \sum_q \int_0^{\mu_q} n_q(T, \mu) d\mu$$

The results will be depicted in Yi Lu's talk.

¹private comm. with N. Wink and J. M. Pawłowski

²P. Isserstedt, C.S. Fischer and T. Steinert, PRD103 (2021) 054012

³**FG**, Yuxin Liu, PRD 94 (2016) 9, 094030

⁴H. Chen, M. Baldo, G. F. Burgio, and H.-J. Schulze, PRD86(2012)045006

Determining the evolution of universe

The idea of leptogenesis is to initially create an asymmetry in the less constrained leptonic sector and transfer this lepton asymmetry into a baryon asymmetry:

- CMB measurements on the baryon asymmetry:
 $b = (8.7 \pm 0.06)^{-11}$ (N. Aghanim et al. (Planck), arXiv: 1807.06209 (2018));
- Observational constraints from big bang nucleosynthesis (BBN) and the CMB on the value of the lepton asymmetry allow values of the lepton asymmetry as large as $|l| < 1.2 \times 10^{-2}$, i.e. around 8 – 9 orders of magnitude larger. (M. Wygas, I. Oldengott, et al, PRL 121, 201302 (2018).)

¹FG, I. Oldengott, PRL. 128, 131301(2022).

Assuming a homogeneous Universe, five conserved quantities are then: $n_{L_\alpha}/s = l_\alpha$, $n_B/s = b$, and $n_Q/s = q$. The entropy density s fulfills the relation

$Ts(T, \mu) = \epsilon(T, \mu) + p(T, \mu) - \sum_a \mu_a n_a(T, \mu)$, with ϵ the total energy density, p the total pressure, and the sum over conserved charges $a \in \{B, Q, L_\alpha\}$. The five local conservation laws can be written in terms of the particle net number densities,

$$l_\alpha s = n_\alpha + n_{\nu_\alpha} ,$$

$$bs = \sum_i B_i n_i ,$$

$$qs = \sum_i Q_i n_i ,$$

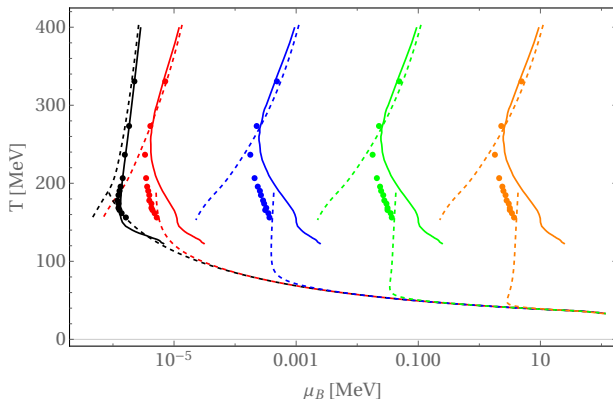
we focus on the following choices for lepton asymmetries l_α during the QCD epoch, Cases (ii)-(vii) were chosen such that the total lepton asymmetry $l = l_e + l_\mu + l_\tau$ always fulfills the CMB constraints.

- (i) $l_e = l_\mu = l_\tau = \frac{l}{3}$ (equilibrated case),
- (ii) $l_e = 0, l_\mu = -l_\tau,$
- (iii) $l_e = -l_\tau, l_\mu = 0,$
- (iv) $l_e = -l_\mu, l_\tau = 0,$
- (v) $l_e = l_\mu, l_\tau = -2l_e$
- (vi) $l_e = l_\tau, l_\mu = -2l_e$
- (vii) $l_e = -2l_\mu, l_\mu = l_\tau$

Values of the lepton asymmetry for which either the u (left column) or the d quark (right column) experience a first-order transition.

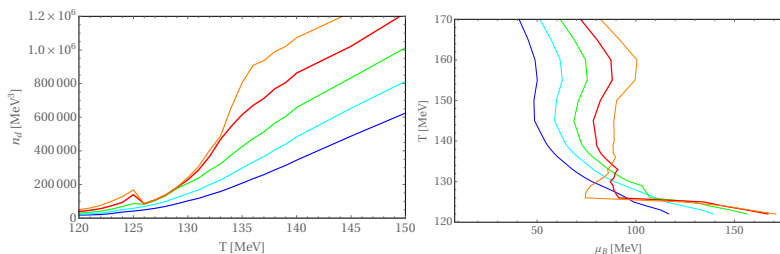
	$\mu_u \geq 111 \text{ MeV}$	$\mu_d \geq 111 \text{ MeV}$
(i)	$l \geq 1.10 \times 10^{-1}$	$l \leq -1.03 \times 10^{-1}$
(ii)	$l_\mu \geq 7.43 \times 10^{-2}$	$l_\mu \leq -6.85 \times 10^{-2}$
(iii)	$l_e \geq 7.1 \times 10^{-2}$	$l_e \leq -6.59 \times 10^{-2}$
(iv)	$l_e \geq 1.36 \times 10^{-3}$	no solution
(v)	$l_e \geq 3.46 \times 10^{-2}$	$l_e \leq -3.23 \times 10^{-2}$
(vi)	$l_e \leq -1.199012 \times 10^{-1}$	$l_e \geq 1.02 \times 10^{-1}$
(vii)	$l_e \leq -1.14 \times 10^{-1}$	$l_e \geq 9.43 \times 10^{-2}$

Temperature evolution of chemical potentials for different negative total lepton asymmetries I .



- low chemical potential, consistent with other results
- the deviation is mostly due to the phase transition line.

Temperature evolution with first order phase transition:



- a kink in the number density;
- discontinuity in the trajectory.

Lepton Asymmetry can induce cosmic QCD first order phase transition, and can be detected via the gravitational wave experiments.

In the future:

- Incorporating the EoS of QCD into hydrodynamics simulations;
- Studying the global properties of QCD matter generated in HIC, for instance, the transport coefficients and the polarization structure.
- Investigating the spectral function of QCD states at finite T and μ .
- Improving the estimation of Cosmic QCD Phase structure;
- Impact on the observables of gravitational waves and also productions of exotic relics (Primordial Black Holes)

Thank you!

Thermal hadrons

To understand deeper on QCD states, the spectrum of QCD matter at finite temperature is important.

Hadrons at finite temperature

The practical way of computing BSEs for mesons at finite temperature is through the imaginary time formula which is simply to change the fourth component of all the momentum in Euclidean space to Matsubara frequency:

$$\lambda(\vec{P}^2, \Omega_m^2) \Gamma_{\pi, \rho}^{ab}(k; P) = T \sum_n \int \frac{d^3 q}{(2\pi)^3} g^2 D_{\mu\nu}(k - q; T) \times \gamma_\mu \chi_{\pi, \rho}^{ab}(q; P) \gamma_\nu, \quad (5)$$

¹FG and Minghui Ding. Eur.Phys.J.C 80 (2020)12, 1171.

Pole and screening mass of hadron at finite temperature

- screening mass M_{scr} via putting $\Omega_m^2 = 0$, extending \vec{P} into complex plane and then locating the screening mass at $\lambda(-M_{\text{scr}}^2, 0) = 1$.
- the pole mass is in principle difficult to define since an analytic continuation of the Matsubara frequency in the form of spectral representation is required:

$$\frac{1}{\Omega_m^2 + \vec{P}^2 + M^2(\vec{P}^2, \Omega_m^2)} = \int_{-\infty}^{\infty} d\omega \frac{\rho(\vec{P}, \omega)}{\omega - i\Omega_m}. \quad (6)$$

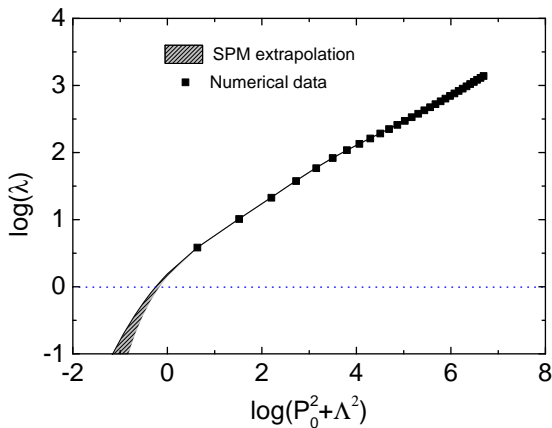
The pole mass is located at $\lambda(\vec{P} = 0, P^2 = -M_{\text{pole}}^2) = 1$ through replacing $i\Omega_m$ with M_{pole} in the above spectral representation. Therefore, if people try to obtain the pole mass directly, the BSE in real time formula with the spectral representation is required.

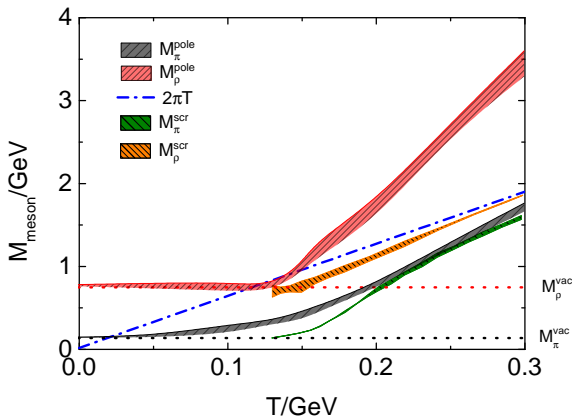
A novel method of computing pole mass

A novel method of computing pole mass:

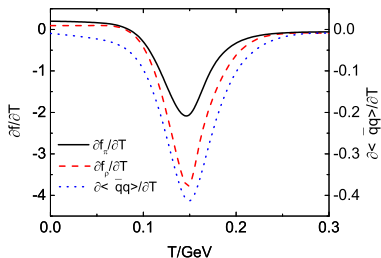
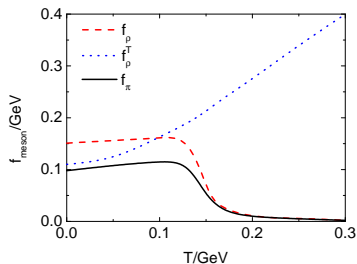
We compute the eigenvalues $\lambda(P^2 = \Omega_m^2)$ at each Ω_m with $m = 1, 2, \dots, m_{\text{Max}}$, and extrapolate them to obtain the pole mass of the meson $M_{\pi,\rho}$ at $\lambda(P^2 = -M_{\pi,\rho}^2) = 1$.

Based on the similar consideration to apply this extrapolation, ie, the extrapolation can work because we know the eigenvalue of Bethe-Salpeter equation increases smoothly and monotonously from 0 to 1, as P_0^2 goes from positive to the on-shell pole mass $P_0^2 = -M_{\text{pole}}^2$.

An example of extrapolation for π pole mass at $T = 150$ MeV



- At low temperature, π pole mass increases monotonously, ρ pole mass at T_S has reached the vacuum value.
- At high temperature, π pole mass gets close to the free field limit above the critical temperature, while the ρ meson pole mass is twice as large as this limit.



- monotonous increase for f_ρ^T
- similar behavior for f_π and f_ρ
- f_π and f_ρ can be considered as the criterion of phase transition.